NASA

TECHNICAL MEMORANDUM

X-525

A SIMPLIFIED METHOD FOR ESTIMATING SUBSONIC LIFT-CURVE SLOPE AT LOW ANGLES OF ATTACK FOR IRREGULAR PLANFORM WINGS

By Bernard Spencer, Jr.

Langley Research Center
Langley Field, Va.

NATIONAL AERONAUTICS AND SPACE ADMINISTRATION

WASHINGTON

May 1961

NATIONAL AERONAUTICS AND SPACE ADMINISTRATION

TECHNICAL MEMORANDUM X-525

A SIMPLIFIED METHOD FOR ESTIMATING SUBSONIC LIFT-CURVE SLOPE AT LOW ANGLES OF ATTACK FOR IRREGULAR PLANFORM WINGS*

By Bernard Spencer, Jr.

SUMMARY

A simplified method is presented for estimating the lift-curve slope of irregular planform wings at subsonic speeds and low angles of attack. The present process is an extension of the method derived in NACA Technical Note 3911 and enables quick estimates of subsonic lift-curve slope to be made whereas more refined procedures require considerable time and computation. Comparison of experimental and estimated values for a wide range of wing planforms having discontinuous spanwise sweep variation indicates good agreement. A comparison of the present procedure with a 20-step vortex method (NACA Research Memorandum L50L13) indicated good agreement for a variable-sweep configuration.

INTRODUCTION

A major problem associated with supersonic aircraft, and hypersonic aircraft considered as possible reentry vehicles, is the fact that the configuration most desirable for the supersonic cruise or the atmospheric reentry is incompatible with subsonic flight and landing requirements. One method of alleviating this problem is the use of variable wing geometry. For high-performance supersonic aircraft, both military (refs. 1 and 2) and commercial (ref. 3), variable-wing sweep offers a possible means of obtaining an aircraft which is efficient at both supersonic and subsonic speeds. With regard to hypersonic aircraft considered as possible reentry configurations, employment of variable geometry such as folding wing-tip panels allows a high-drag, high Mach number atmospheric reentry maneuver to be accomplished while still maintaining desirable glide angles in the approach conditions (refs. 4 and 5).

*Title, Unclassified.

Since one of the major purposes of variable geometry is to provide lift effectiveness at subsonic speeds, a rapid method of estimating the lift-curve slope at subsonic speeds for configurations having variable-geometry wing planforms would be desirable for preliminary design study purposes. For the most part the wings, when in the low-speed position, are of unconventional planform and although various methods such as those of references 6, 7, and 8 can be used in estimating the lift-curve slope for these planforms, they are quite involved and laborious. The method of reference 9 provides a simple means for estimating subsonic lift-curve slope at low angles of attack for wings with constant sweep along the span. The purpose of the present report is to extend the method of reference 9 to include wings having variation in sweep along the span.

SYMBOLS

A	aspect ratio, b^2/S
a_o	section lift-curve slope, per deg
b	wing span, ft
c	wing chord, ft
$\bar{c}$	mean aerodynamic chord, ft
C_L	wing lift coefficient
C_{L_α}	wing lift-curve slope, per deg
M	free-stream Mach number
S	wing area, sq ft
x	longitudinal coordinate of wing leading edge, ft (fig. 1)
y	lateral coordinates as referenced to wing root chord, ft
λ	taper ratio
$\Lambda_{c/2}$	sweep of half-chord line, deg
Λ_{LE}	sweep of leading edge of outboard wing panel, deg

$\Lambda_{LE,in}$ sweep of inboard or fixed portion of wing as referenced from wing root chord, deg

Subscripts:

av	average
i	incremental
eff	effective
LE	leading edge
r	root

DEVELOPMENT OF THE METHOD

The equation derived by Polhamus (see eq. (A7) of ref. 9) for predicting the subsonic lift-curve slope of a constant-sweep finite wing is (for $a_o = 2\pi$)

$$C_{L_\alpha} = \frac{2\pi A}{2 + \sqrt{4 + \left(\frac{A}{\cos \Lambda_{c/2}}\right)^2 - (AM)^2}} \frac{1}{57.3} \qquad (1)$$

This equation takes into account the effects of compressibility, wing sweep, and aspect ratio for wings on which the span loading is approximately elliptical. Use of the half-chord line, as the sweep reference line, eliminates to a large extent, the effects of taper. (See ref. 9.) Equation (1) is a simple means for estimating lift-curve slopes for wings having constant sweep, but does not directly apply to irregular planform wings, such as variable-sweep configurations. An extension of equation (1) to unconventional planforms appears to be possible by use of an effective value of $\cos \Lambda_{c/2}$, provided the span-load distribution is approximately elliptical.

An effective value of $\cos \Lambda_{c/2}$ which has been found to be satisfactory in predicting lift-curve slopes is a weighted average of the local value of $\cos \Lambda_{c/2}$ in which the local chord length is used as a weighting factor. Standard procedure for obtaining the weighted average of a number of quantities is to multiply each quantity by its weighting factor and divide the sum of these products by the sum of the weighting factors. Application of this rule to determine an

effective value of $\cos \Lambda_{c/2}$ may be done by dividing the wing into N sections, each section being assumed to have constant-sweep angles within its boundary.

The span of section i is denoted by Δy_i, the average chord of section i, by $c_{av,i}$, and the cosine of the sweep angle of the half-chord line of section i, by $(\cos \Lambda_{c/2})_i$. The weighted average or effective value of $\cos \Lambda_{c/2}$ is therefore defined as

$$(\cos \Lambda_{c/2})_{eff} = \frac{\sum_{i=1}^{i=N} (\cos \Lambda_{c/2})_i c_{av,i} \Delta y_i}{\sum_{i=1}^{i=N} c_{av,i} \Delta y_i} \qquad (2)$$

The denominator of equation (2) is the total area of one wing panel $S/2$. Therefore, equation (2) may be written as follows:

$$(\cos \Lambda_{c/2})_{eff} = \frac{2}{S} \sum_{i=1}^{i=N} (\cos \Lambda_{c/2})_i c_{av,i} \Delta y_i \qquad (3)$$

The value of $(\cos \Lambda_{c/2})_{eff}$ may be determined from the wing geometry and substituted into equation (1) for $\cos \Lambda_{c/2}$. Equation (1) then becomes

$$C_{L_\alpha} = \frac{2\pi A}{2 + \sqrt{4 + \left[\frac{A}{(\cos \Lambda_{c/2})_{eff}}\right]^2 - (AM)^2}} \left(\frac{1}{57.3}\right) \qquad (4)$$

RESULTS AND DISCUSSION

In order to evaluate the accuracy of the present method in estimating lift-curve slopes at subsonic speeds, a comparison of experimental

results with the method derived in this paper is presented for a wide range of planforms having variations in sweep along the span.

Figure 1 presents geometric characteristics for several low-aspect-ratio planforms which have been considered as possible hypersonic or reentry vehicles. Data for wings 1, 2, 5, and 6 are presented in references 4 and 5, and data for wings 3, 4, and 7 are from unpublished results. Figure 2 presents comparisons of the experimental and estimated values of lift coefficient plotted against angle of attack for the wings of figure 1. Reasonable correlation between the experimental and the estimated values exists at low angles of attack for all wing planforms except wing 6. (This fact may be seen in fig. 3, which presents the correlation of experimental and estimated values of C_{L_α} at $\alpha = 0^\circ$.) The method appreciably underestimates lift-curve slope above $\alpha = 6^\circ$ to 8° for wings 1 to 7.

Figure 4 presents the experimental and estimated values of lift-curve slope plotted against Mach number for wings 1, 2, 5, and 6 at $\alpha = 0^\circ$. Comparisons of experimental values of C_{L_α} with estimates of the present method indicate poorer correlation as the Mach number approaches 1.0 for wings 5 and 6 which are the higher-aspect-ratio configurations.

Figure 5 presents the geometric characteristics of the airplane configuration of reference 10, herein designated as configuration I, and figure 6 presents the variation of lift coefficient with angle of attack for this configuration. Estimated values of lift coefficient were made by the present method and the method of reference 7. Good correlation with experiment at the lower angles of attack is noted for the present method with some improvement over the estimates of reference 7. Figure 7 presents the variation of lift-curve slope with Mach number for configuration I, and this plot indicates underestimation by use of the present method of determining C_{L_α} as the Mach number approaches 1.0.

Figure 8 presents the geometric characteristics of the basic outboard-tail arrangement of reference 11, herein designated as configuration II, and figure 9 presents a comparison of the experimental and estimated values of lift coefficient plotted against angle of attack for this arrangement. In determining the total aspect ratio and in estimating the lift-curve slope of configuration II, the horizontal tail was considered as part of the wing. Exceptionally good agreement at low lift coefficients between the experimental and estimated values is noted for this configuration.

Extreme cases of irregular planform wings are those involving variable-sweep geometry. These configurations essentially have fixed portions of the wing inboard and employ sweeping of the outer portions as a method of combating off-design penalties encountered at subsonic speeds. Figure 10 presents the geometric characteristics of one of the models of reference 1, which is referred to herein as configuration III, and figure 11 presents a comparison of the experimental and estimated values of lift coefficient plotted against angle of attack for three of the wing-sweep positions tested. Figure 12 presents comparisons of the experimental and estimated values of lift-curve slope plotted against leading-edge sweep angle of the outboard portion of the wing of configuration III at $M = 0.25$. Good prediction of C_{L_α} is noted throughout the sweep range, except for the case of 0° leading-edge sweep, where the experimental value is lower than the estimated value.

Geometric characteristics of the variable-sweep configuration of reference 12, herein designated as configuration IV, are presented in figure 13. Figure 14 presents the variation of lift coefficient with angle of attack for this configuration. Figure 15 presents a comparison between the present method and the 20-step method of reference 6 in predicting lift-curve slope for configuration IV. The present method is seen to overestimate C_{L_α} for the configuration throughout the sweep range except for the maximum sweep condition where good correlation is obtained for the low-aspect-ratio configuration. The present method indicates good agreement with the 20-step method throughout the sweep range.

Figure 16 presents a correlation of experimental and estimated values of lift-curve slope for configurations I to IV. This correlation essentially provides a comparison for 11 different planforms having sweep variations across the wing span. The present method is seen to predict the lift-curve slope within ±3 percent for all the configurations presented.

DESIGN CHARTS

It has been determined in reference 9 that C_{L_α}/A is a unique function of $\frac{A}{\cos \Lambda_{c/2}}$ when the section lift-curve slope a_o is considered equal to 2π. Consequently, C_{L_α}/A is also a unique function of $\frac{A}{(\cos \Lambda_{c/2})_{eff}}$, and design charts, similar to those of reference 9,

are presented herein for convenience in determining lift-curve slope. Figure 17 presents the variation of C_{L_α}/A with $\frac{A}{(\cos \Lambda_{c/2})_{eff}}$ for the case of incompressible flow. In order to correct C_{L_α} for the effect of Mach number, correction factors are presented in figure 18 as functions of the effective sweep of the half-chord line for a wide range of aspect ratios.

CONCLUDING REMARKS

A simplified method is presented for estimating the subsonic lift-curve slope of irregular planform wings at low angles of attack. The present process is an extension of the method developed in NACA Technical Note 3911. Comparisons of experiment and estimates for a wide range of configurations having wing planforms with discontinuous spanwise sweep variation indicated good agreement near zero angle of attack. Comparisons of the present method with other existing methods for predicting lift-curve slopes of irregular planform wings generally indicated good agreement.

Langley Research Center,
National Aeronautics and Space Administration,
Langley Field, Va., February 10, 1961.

REFERENCES

1. Alford, William J., Jr., and Henderson, William P.: An Exploratory Investigation of the Low-Speed Aerodynamic Characteristics of Variable-Wing-Sweep Airplane Configurations. NASA TM X-142, 1959.

2. Polhamus, Edward C., and Hammond, Alexander D.: Aerodynamic Research Relative to Variable-Sweep Multimission Aircraft. Ch. II of Compilation of Papers Summarizing Some Recent NASA Research on Manned Military Aircraft. NASA TM X-420, 1960, pp. 13-38.

3. Toll, Thomas A.: Variable Geometry for Transports. Ch. VIII of The Supersonic Transport - A Technical Summary. NASA TN D-423, 1960, pp. 71-79.

4. Spencer, Bernard, Jr.: An Investigation at Subsonic Speeds of Aerodynamic Characteristics at Angles of Attack From -4° to 100° of a Delta-Wing Reentry Configuration Having Folding Wingtip Panels. NASA TM X-288, 1960.

5. Spencer, Bernard, Jr.: An Investigation at Subsonic Speeds of the Longitudinal Aerodynamic Characteristics at Angles of Attack From -4° to 100° of Delta-Wing Reentry Configurations Having Vertically Displaced and Cambered Wing-Tip Panels. NASA TM X-440, 1961.

6. Campbell, George S.: A Finite-Step Method for the Calculation of Span Loadings of Unusual Plan Forms. NACA RM L50L13, 1951.

7. McLaughlin, Milton D.: Method of Estimating the Stick-Fixed Longitudinal Stability of Wing-Fuselage Configurations Having Unswept or Swept Wings. NACA RM L51J23, 1952.

8. Brebner, G. G.: The Calculation of the Loading and Pressure Distribution on Cranked Wings. R. & M. No. 2947, British A.R.C., 1955.

9. Lowry, John G., and Polhamus, Edward C.: A Method for Predicting Lift Increments Due to Flap Deflection at Low Angles of Attack in Incompressible Flow. NACA TN 3911, 1957.

10. Fournier, Paul G.: Wind-Tunnel Investigation of the High-Subsonic Static Longitudinal Stability Characteristics of Several Wing-Body Configurations Designed for High Lift-Drag Ratios at a Mach Number of 1.4. NACA TN 4340, 1958.

11. Hayes, William C., Jr., and Sleeman, William C., Jr.: Low-Speed Investigation of the Effects of Wing Flap Deflection and Horizontal-Tail Configuration on the Longitudinal Aerodynamic Characteristics of an Airplane Configuration Having Tail Surfaces Outboard of the Wing Tips. NASA TM X-333, 1960.

12. Spencer, Bernard, Jr.: Stability and Control Characteristics at Low Subsonic Speeds of an Airplane Configuration Having Two Types of Variable-Sweep Wings. NASA TM X-303, 1960.

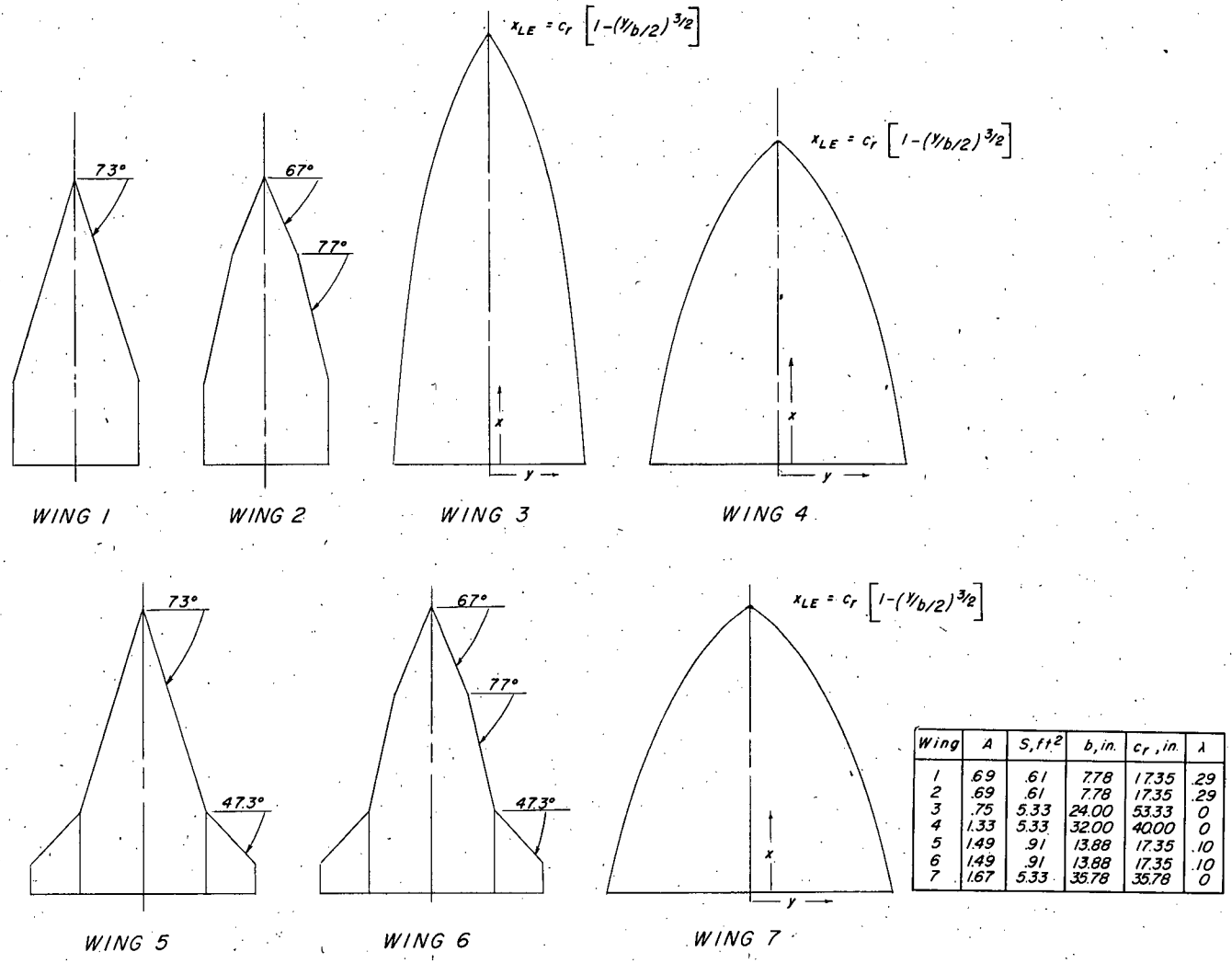

Wing	A	S, ft²	b, in.	c_r, in.	λ
1	.69	.61	7.78	17.35	.29
2	.69	.61	7.78	17.35	.29
3	.75	5.33	24.00	53.33	0
4	1.33	5.33	32.00	40.00	0
5	1.49	.91	13.88	17.35	.10
6	1.49	.91	13.88	17.35	.10
7	1.67	5.33	35.78	35.78	0

Figure 1.- Planform characteristics of several low-aspect-ratio wing configurations considered as possible hypersonic or reentry vehicles.

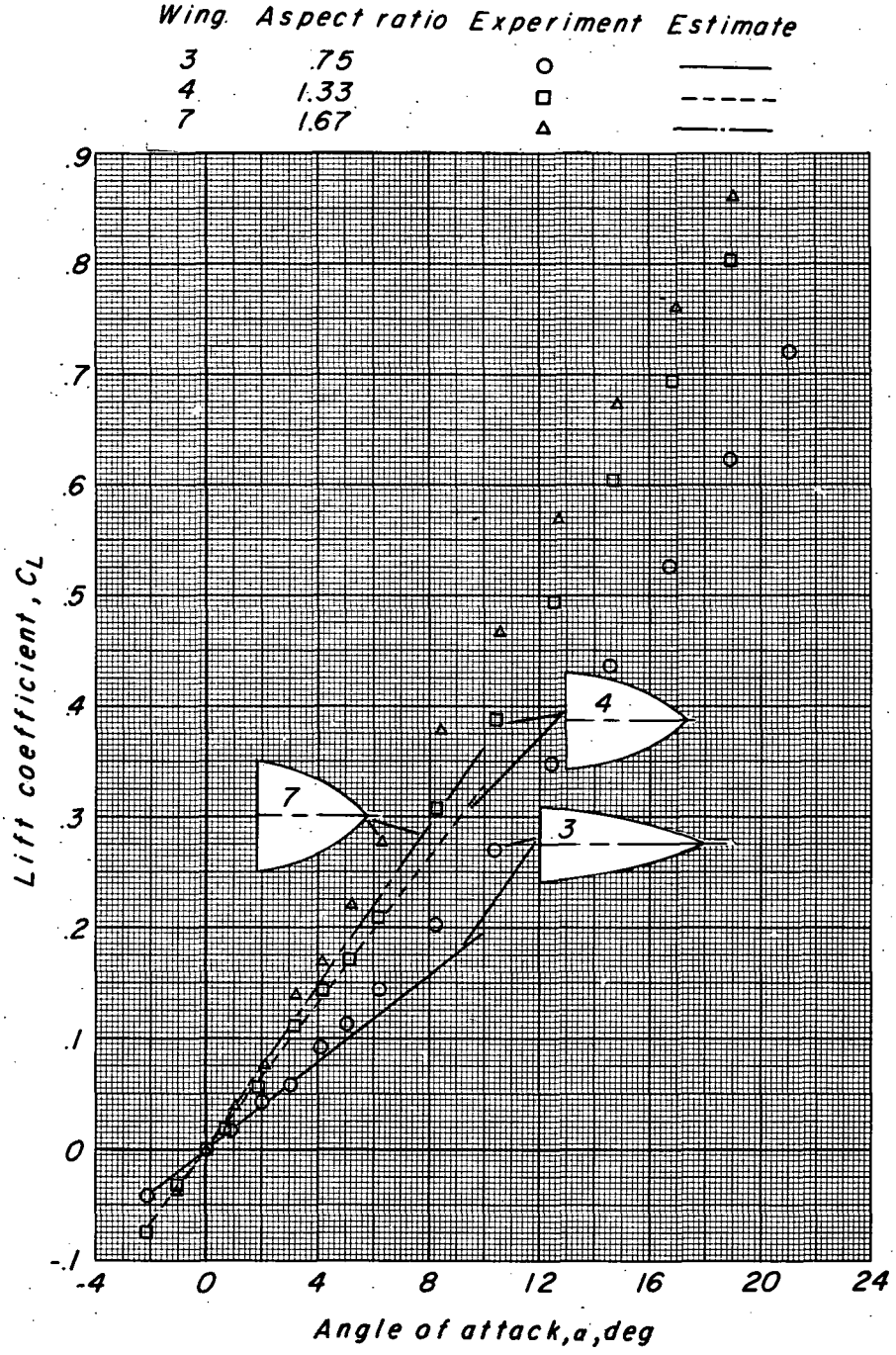

(a) Wings 3, 4, and 7; M = 0.12.

Figure 2.- Comparison of experimental and estimated values of lift coefficient plotted against angle of attack for wings presented in figure 1.

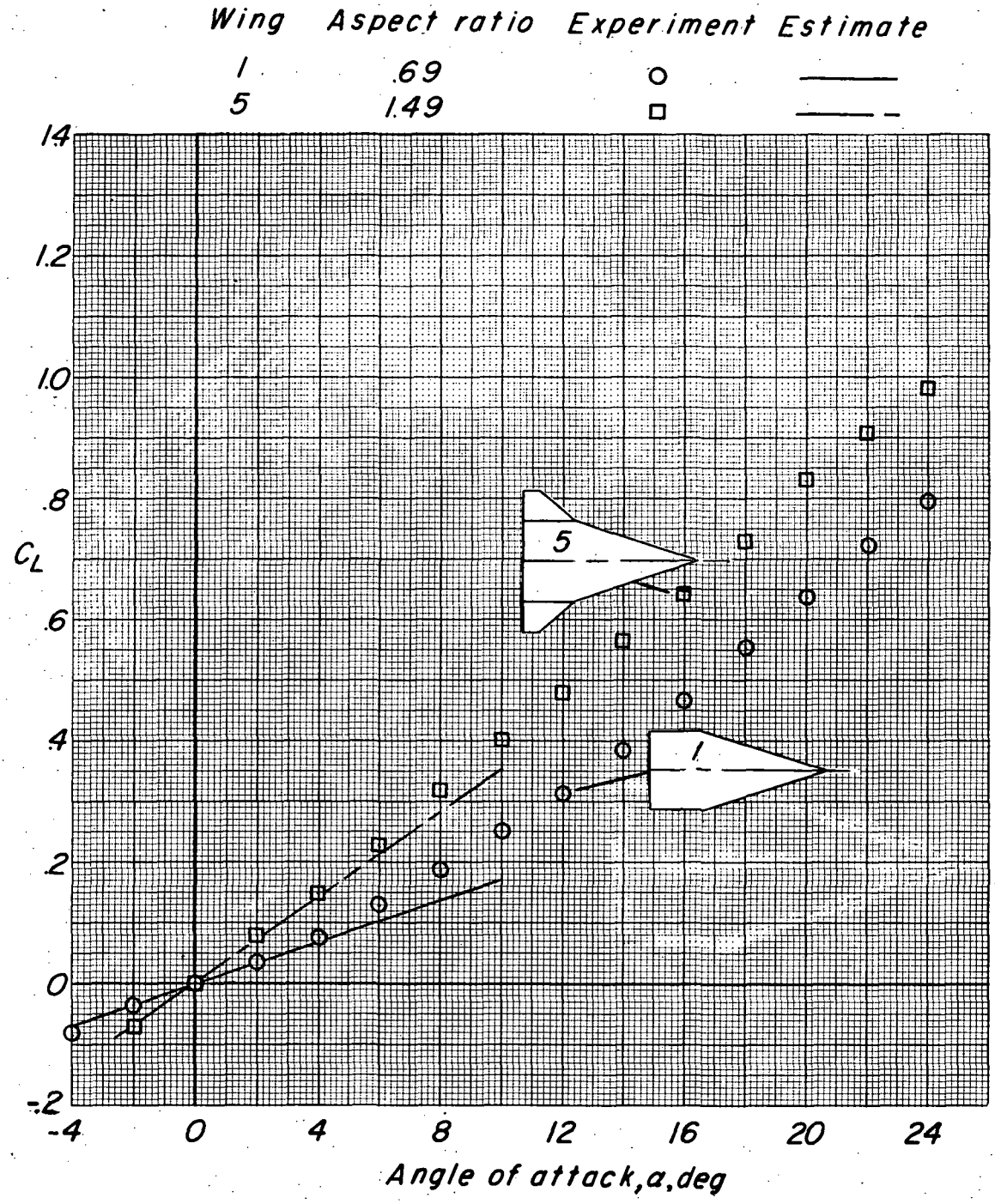

(b) Wings 1 and 5; M = 0.40.

Figure 2.- Continued.

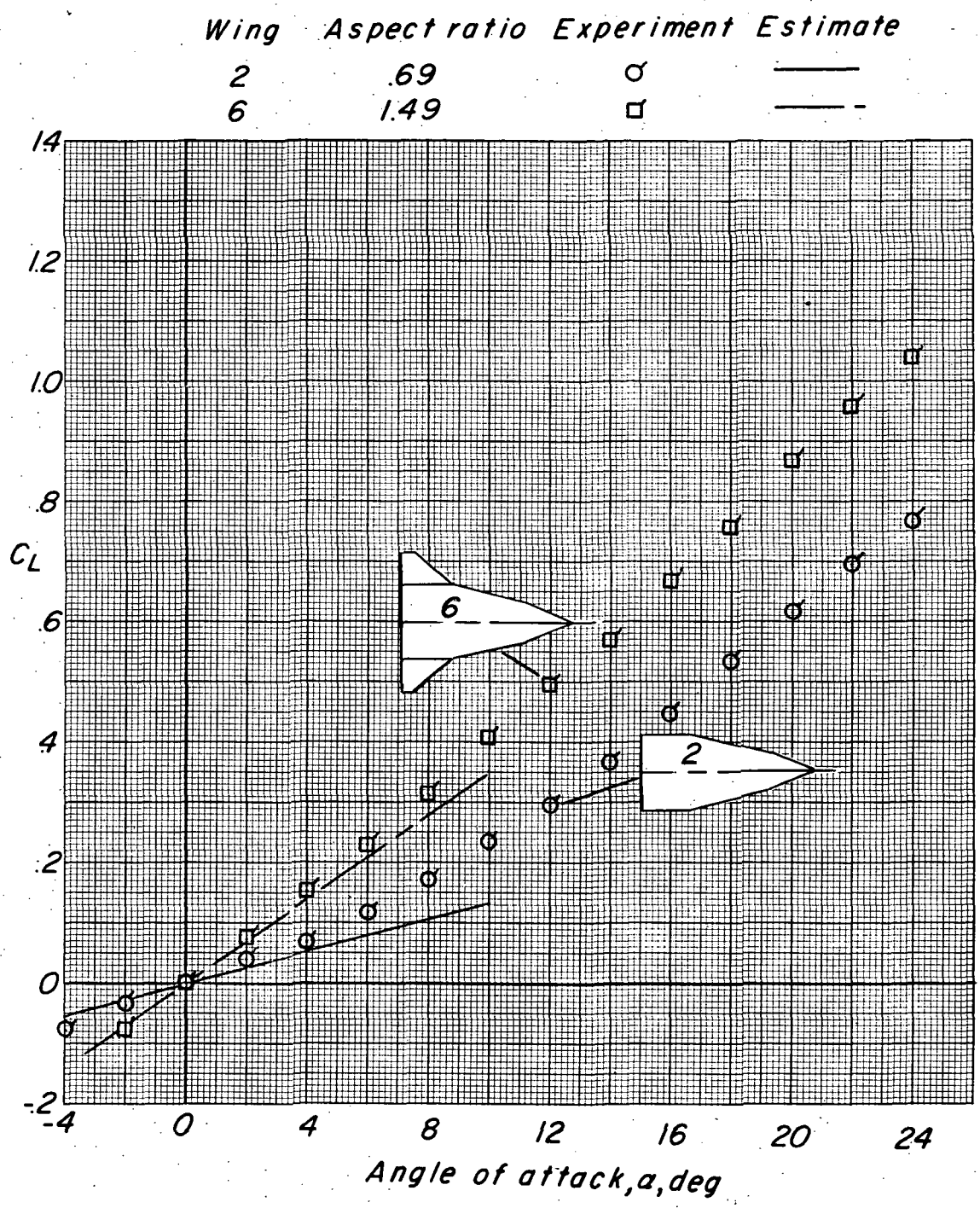

(c) Wings 2 and 6; M = 0.40.

Figure 2.- Concluded.

	Wing no.	Experiment	Estimate	Aspect ratio	Mach no.
○	1	.0175	.0175	.69	.40
□	2	.0170	.0168	.69	.40
◇	3	.0190	.0195	.75	.12
△	4	.0320	.0330	1.33	.12
⊿	5	.0369	.0361	1.49	.40
▫	6	.0374	.0359	1.49	.40
▽	7	.0355	.0360	1.67	.12

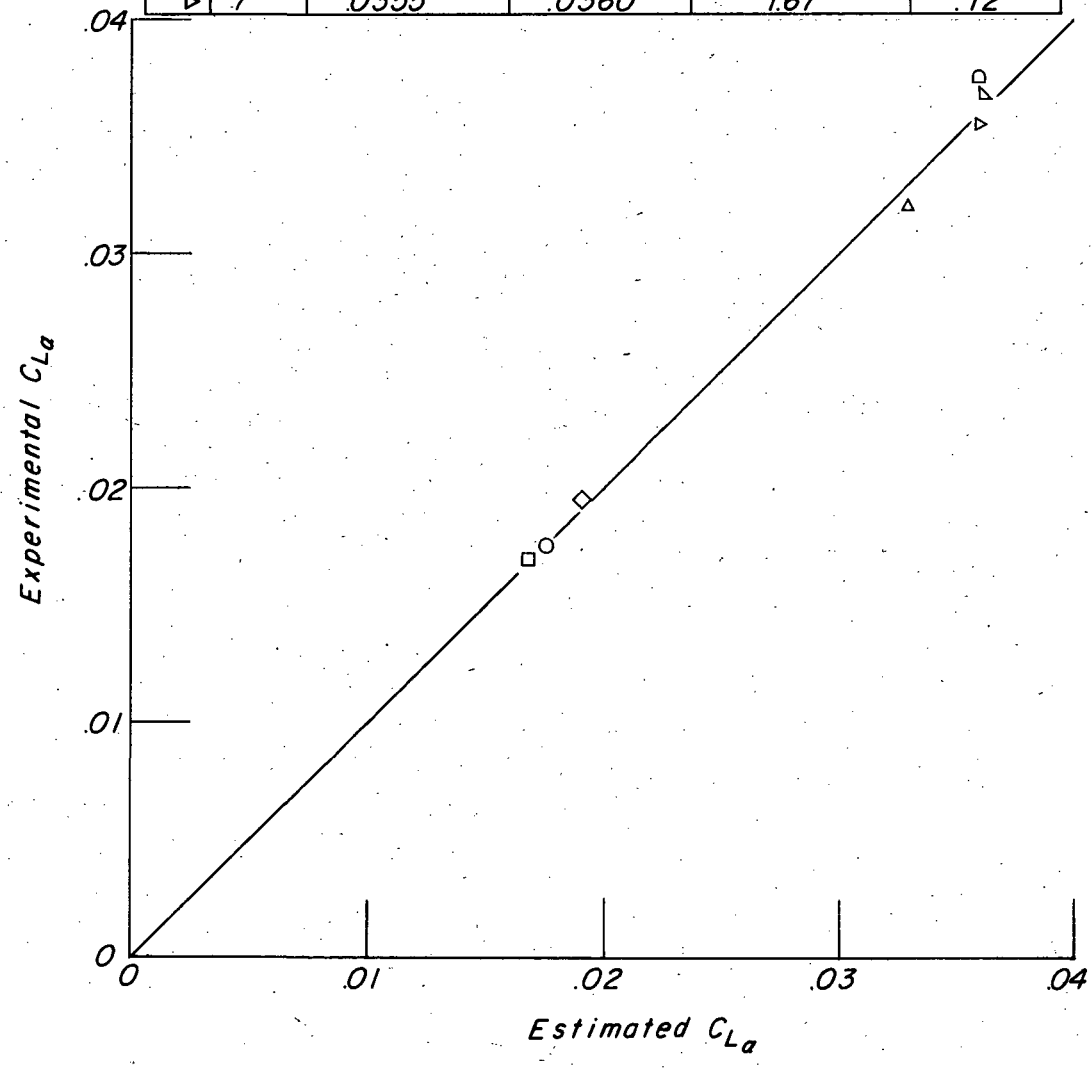

Figure 3.- Correlation of experimental and estimated values of lift-curve slope for low-aspect-ratio wings at $\alpha = 0^{\circ}$.

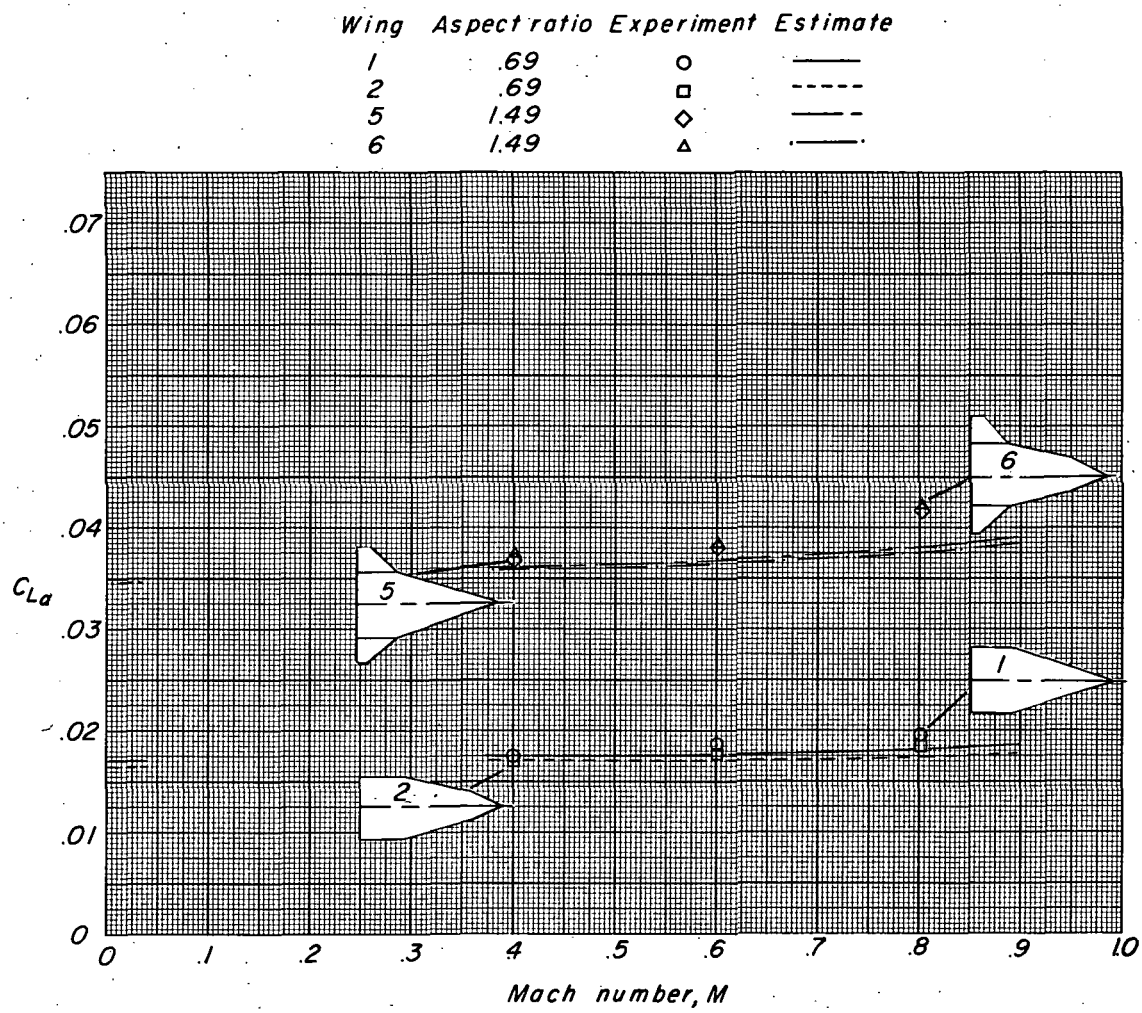

Figure 4.- Comparison of experimental and estimated values of lift-curve slope plotted against Mach number for wings 1, 2, 5, and 6 at $\alpha = 0^\circ$.

L-1321

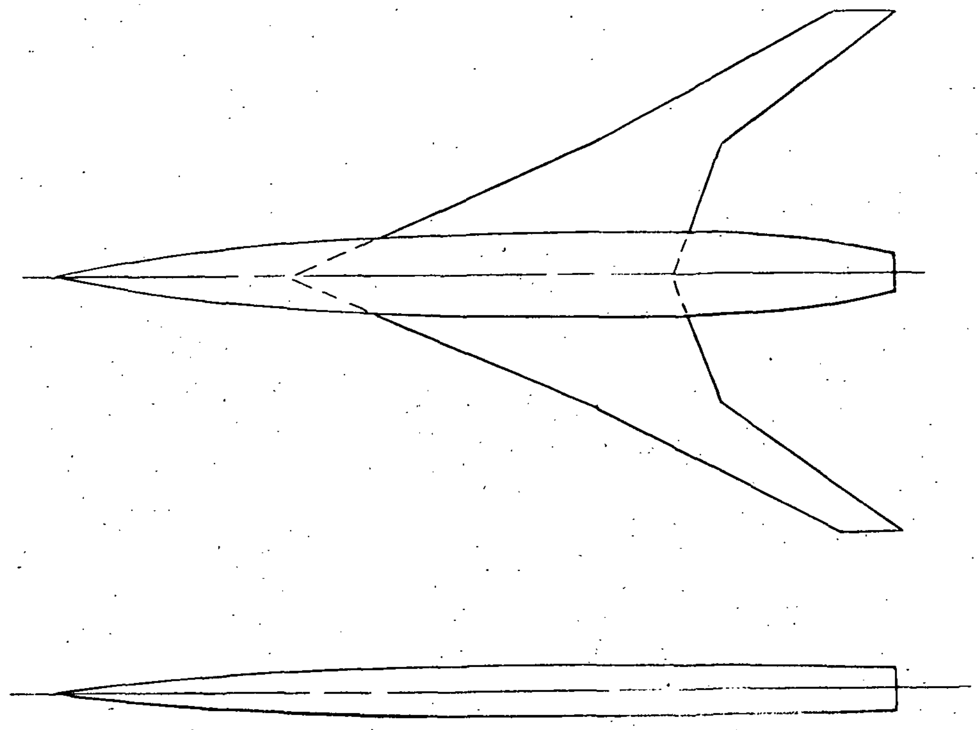

Configuration I

Wing Characteristics

Sweep	L.E.	T.E.
Inboard	67.01°	19.65°
Outboard	61.70°	53.61°
Area, sq ft		1.375
Aspect ratio		2.91
Taper ratio		.167
Mean aerodynamic chord, ft		.895

Figure 5.- Details of model of reference 10 (designated herein as configuration I).

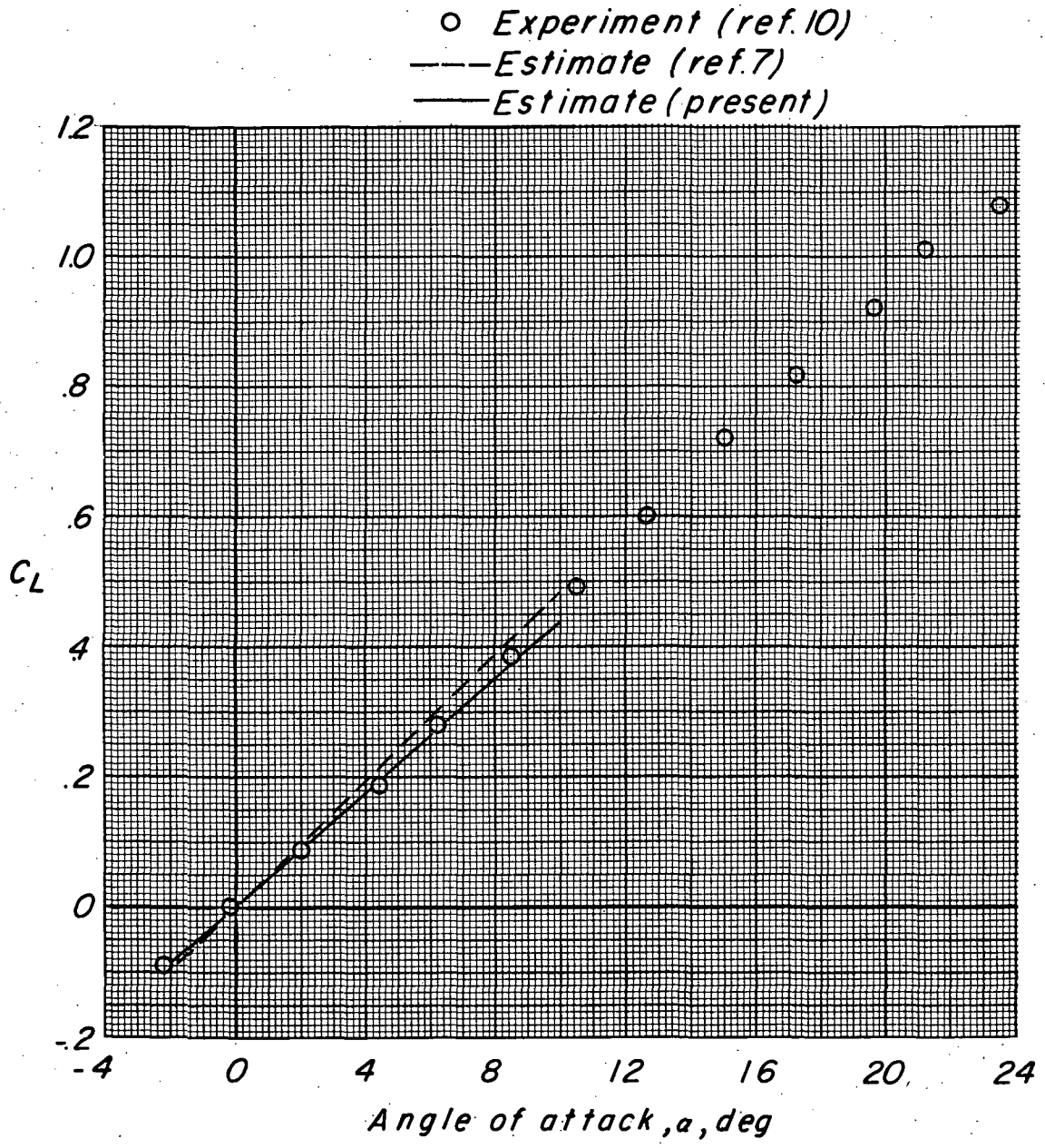

Figure 6.- Variation of lift coefficient with angle of attack of configuration I. M = 0.60.

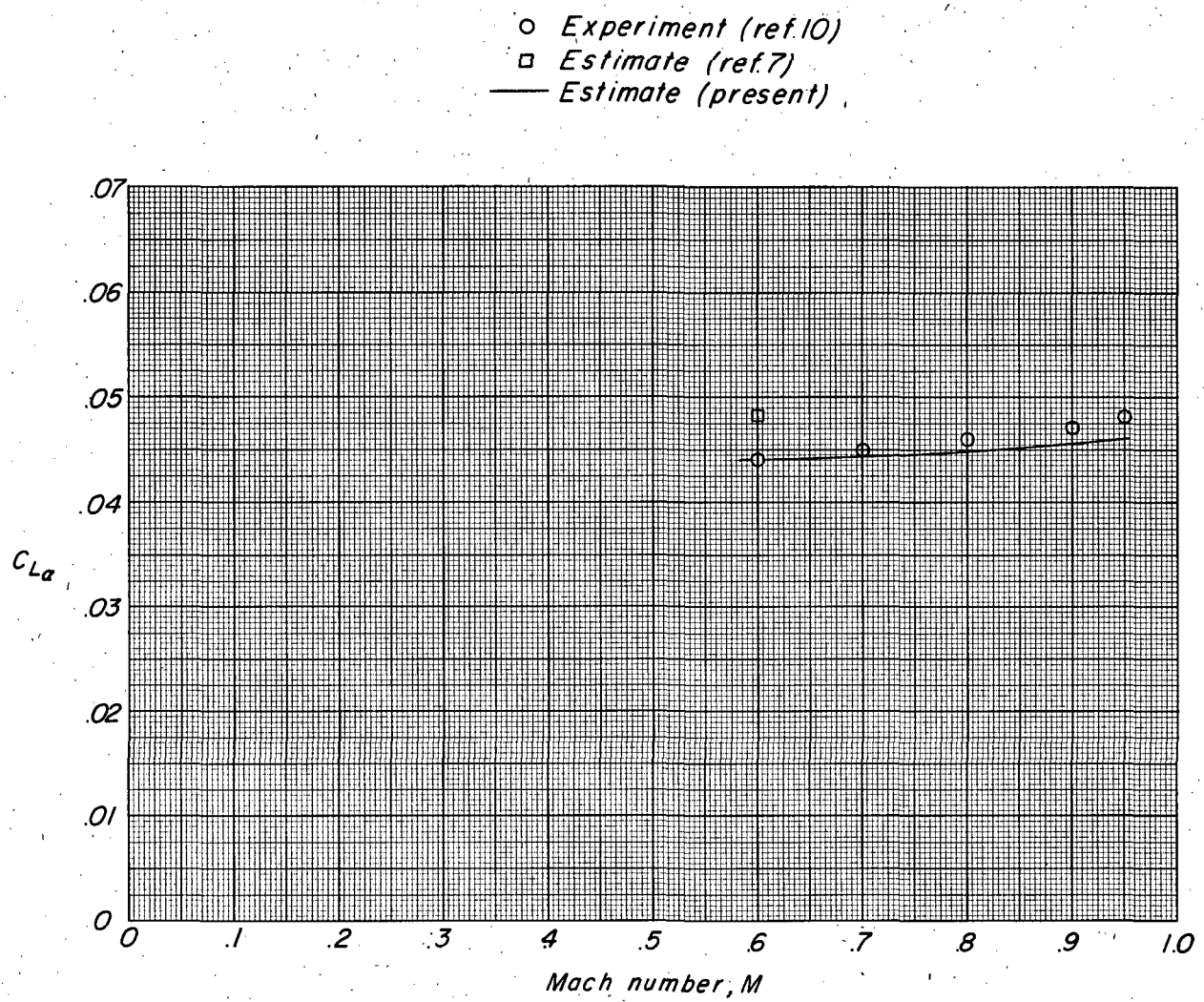

Figure 7.- Comparison of experimental and estimated values of lift-curve slope plotted against Mach number for configuration I at $\alpha = 0^{\circ}$.

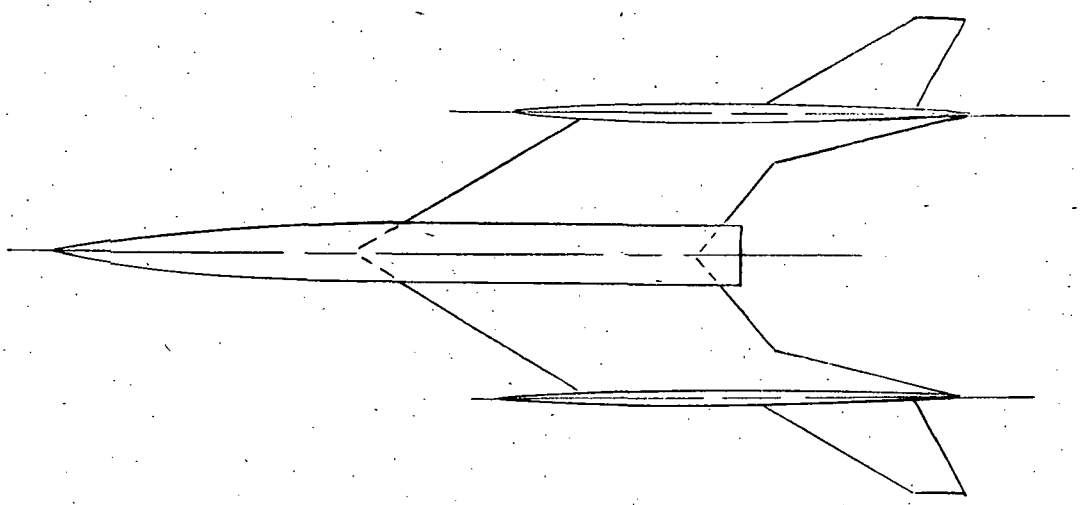

L-1321

Configuration II

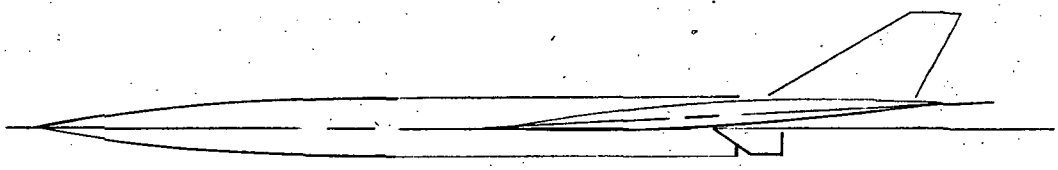

Wing geometry	
Area	784.00 sq in.
Root chord	34.25 in.
Tip chord	21.75 in.
Span	28.00 in.
Aspect ratio	1.00
Tail geometry	
Area (one tail)	100.66 sq in.
Root chord	16.08 in.
Tip chord	5.11 in.
Panel span	9.50 in.

Figure 8.- Details of model of reference 11 (designated herein as configuration II).

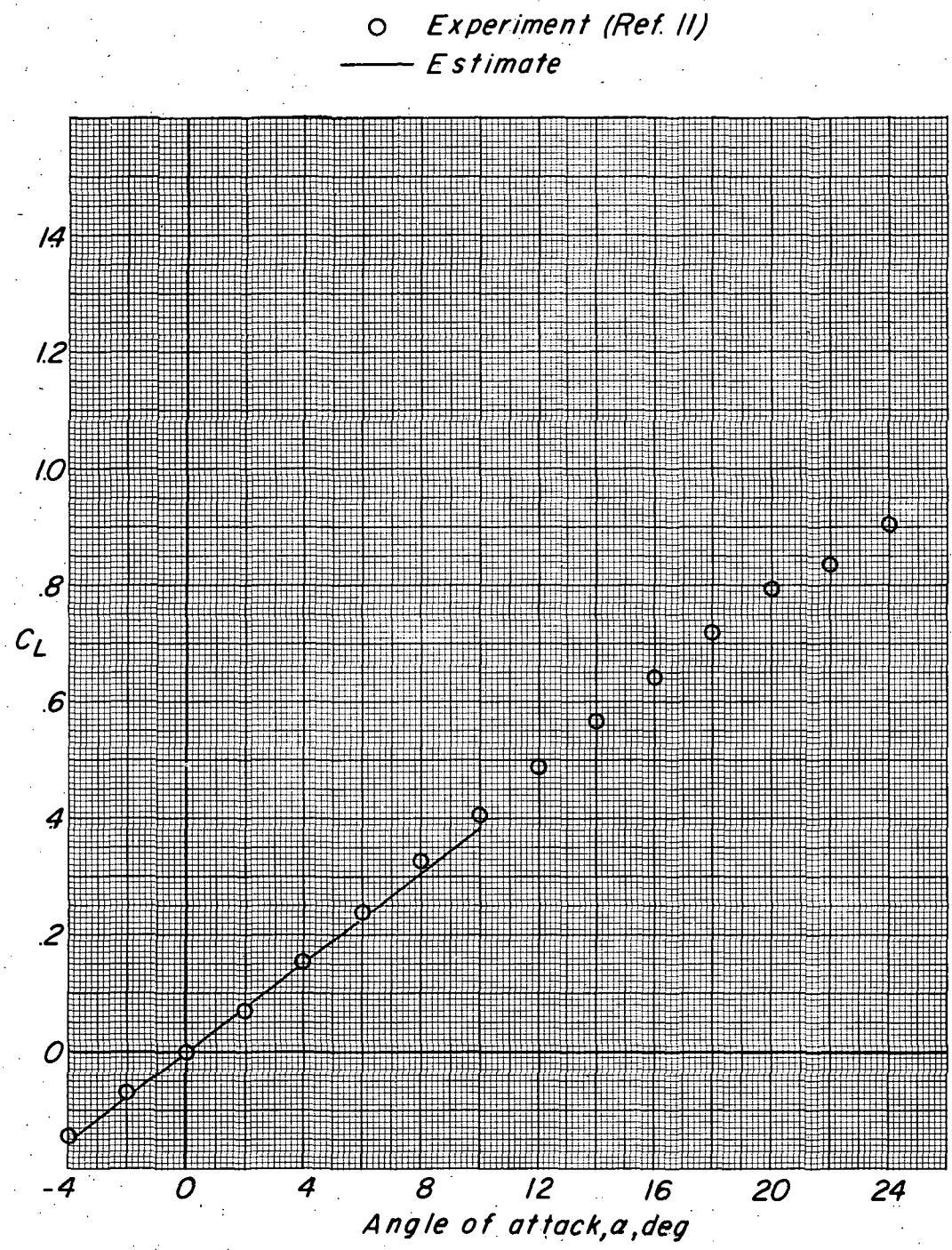

Figure 9.- Comparison of experimental and estimated values of lift coefficient plotted against angle of attack for configuration II. $M \approx 0$.

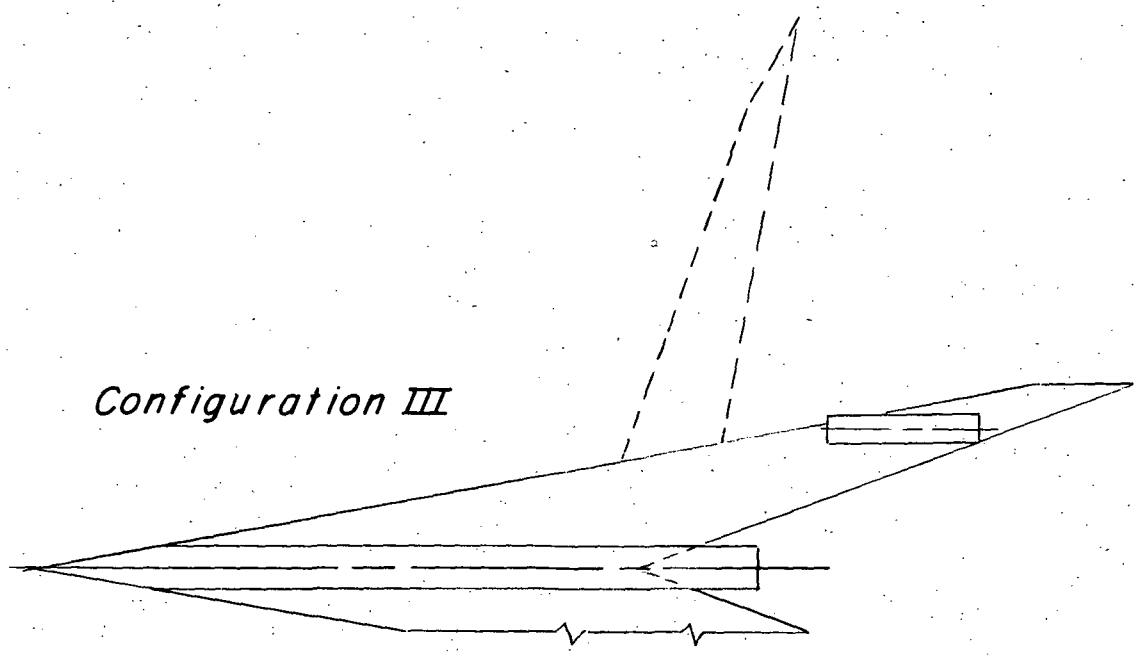

Geometric Characteristics

Airfoil section normal to leading edge	NACA 63_{10}A014
Camber and twist	None
Aspect ratio	
For $\Lambda_{LE}=20°$	10.35
$\Lambda_{LE}=80°$	1.05
Area, sq ft	
For $\Lambda_{LE}=20°$	2.68
$\Lambda_{LE}=80°$	2.65
Reference chord ($\bar{c}$ for $\Lambda_{LE}=80°$), ft	1.865
Moment reference point	0.234 $\bar{c}$

Figure 10.- Details of variable-sweep configuration of reference 1 (designated herein as configuration III).

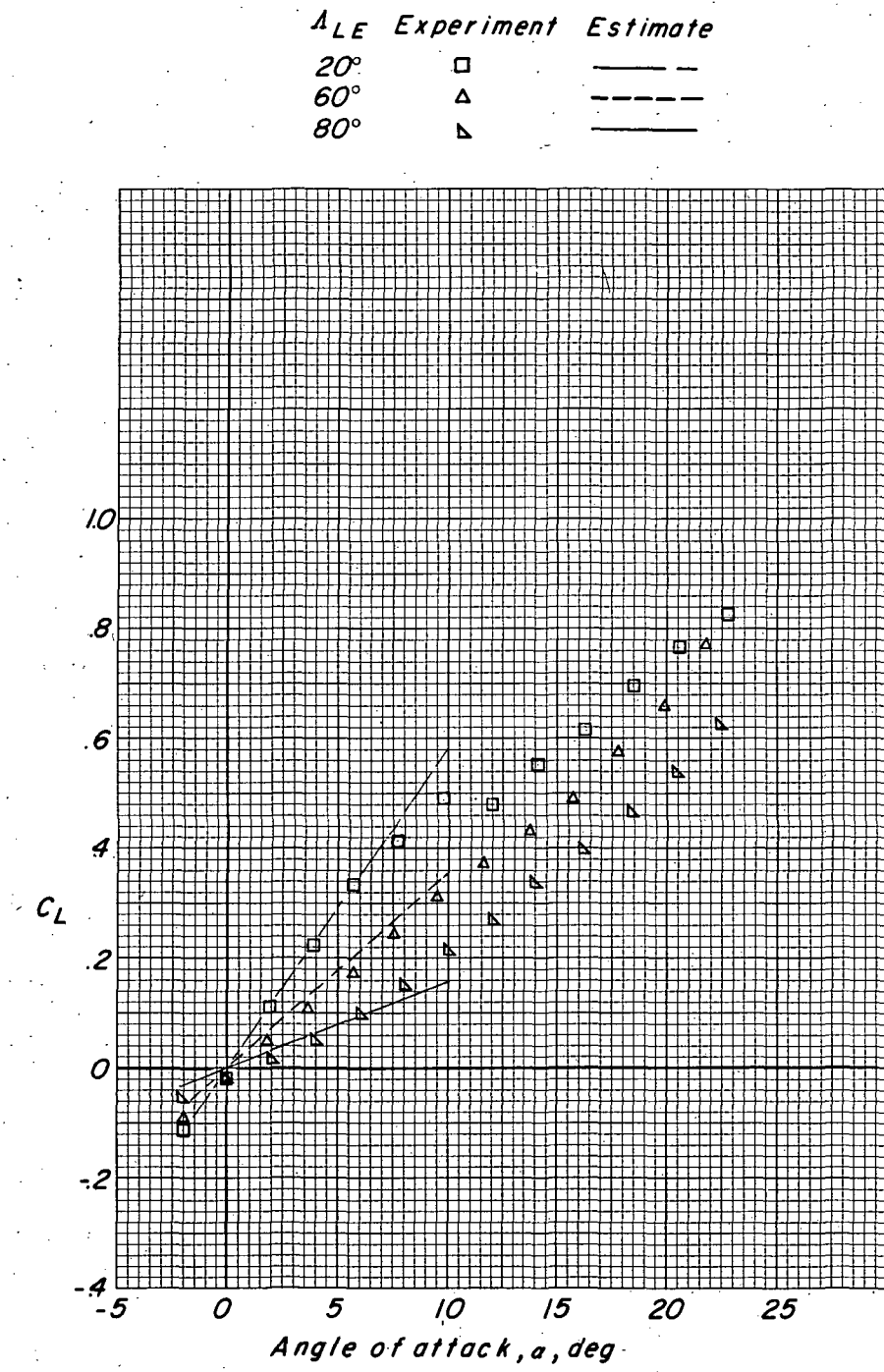

Figure 11.- Comparison of experimental and estimated values of lift coefficient plotted against angle of attack for configuration III at three positions of the outboard wing panel. M = 0.25.

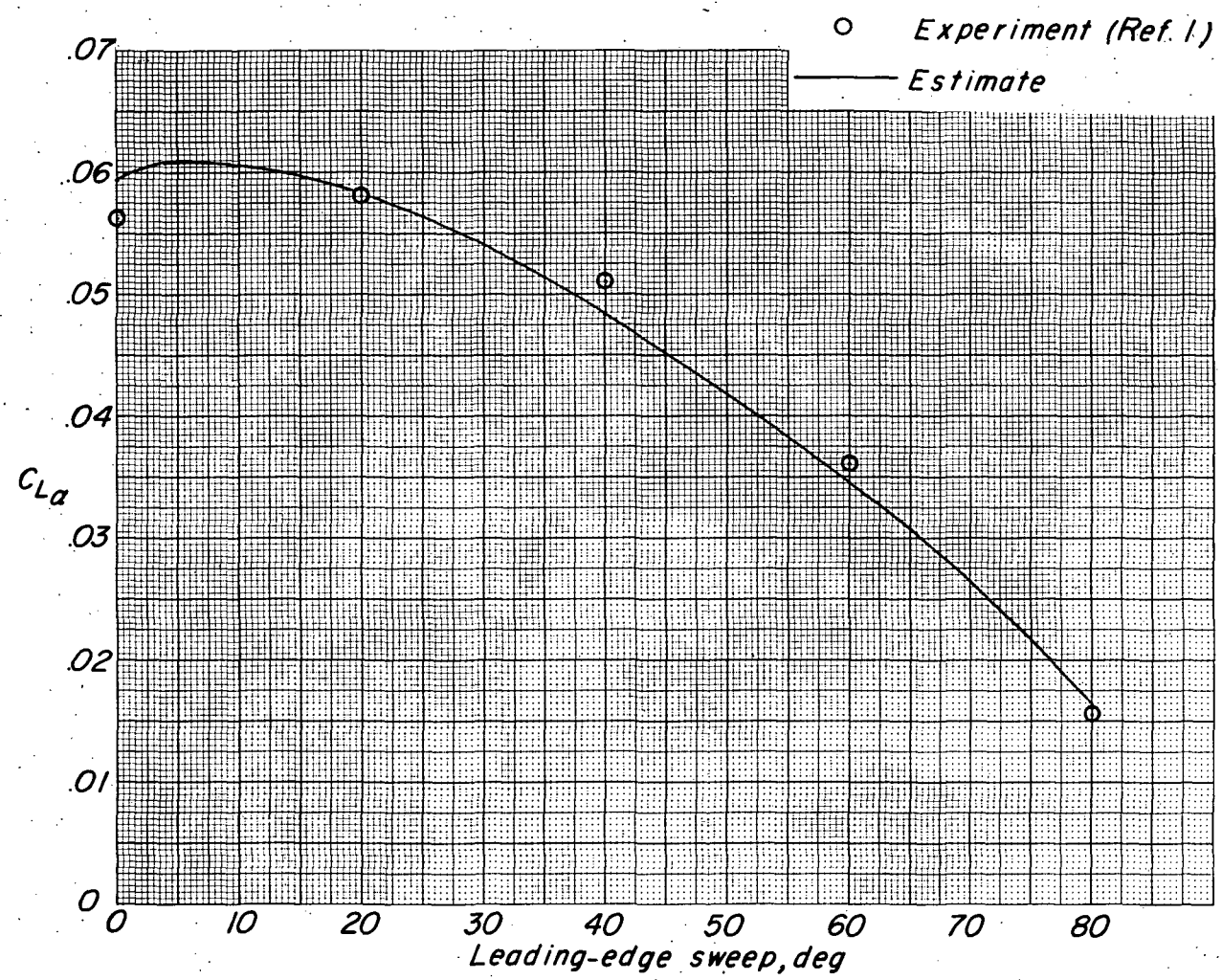

Figure 12.- Comparison of experimental and estimated values of lift-curve slope plotted against leading-edge sweep angle of outboard panel of configuration III. M = 0.25.

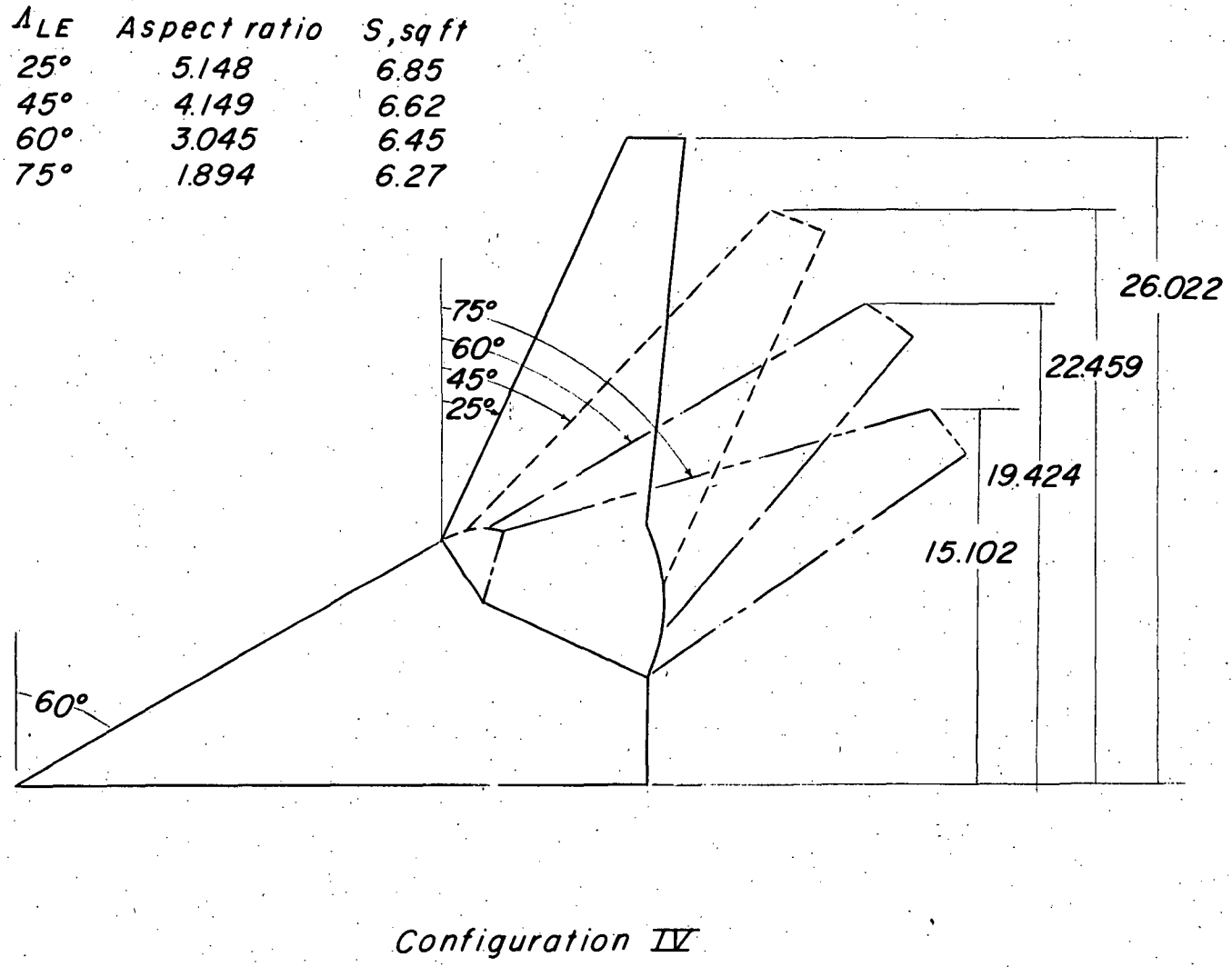

Figure 13.- Details of variable-sweep configuration of reference 12 (designated herein as configuration IV). (All dimensions are in inches unless otherwise noted.)

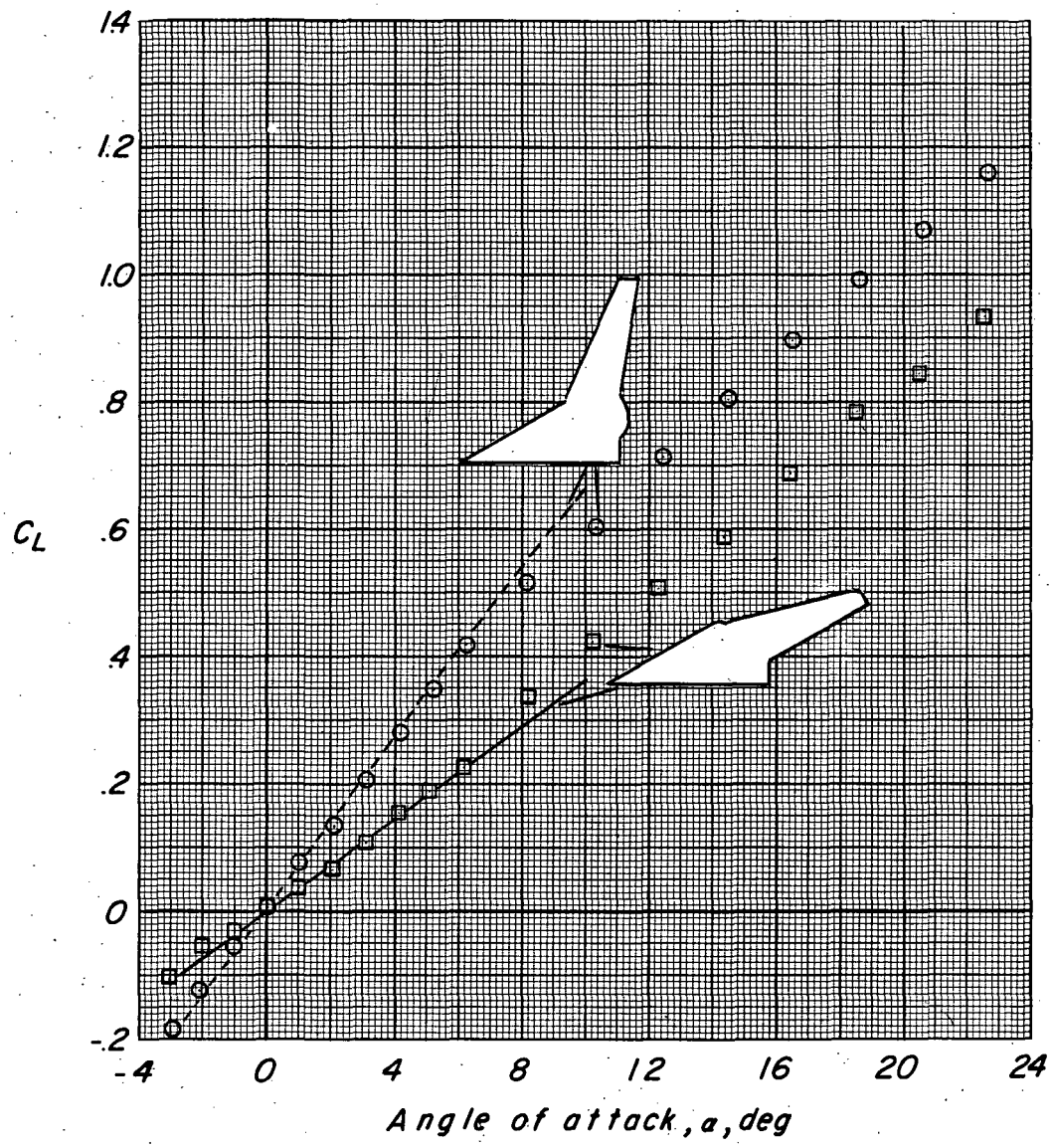

Figure 14.- Comparison of experimental and estimated values of lift coefficient plotted against angle of attack for configuration IV at two positions of the outboard wing panel. $M \approx 0$.

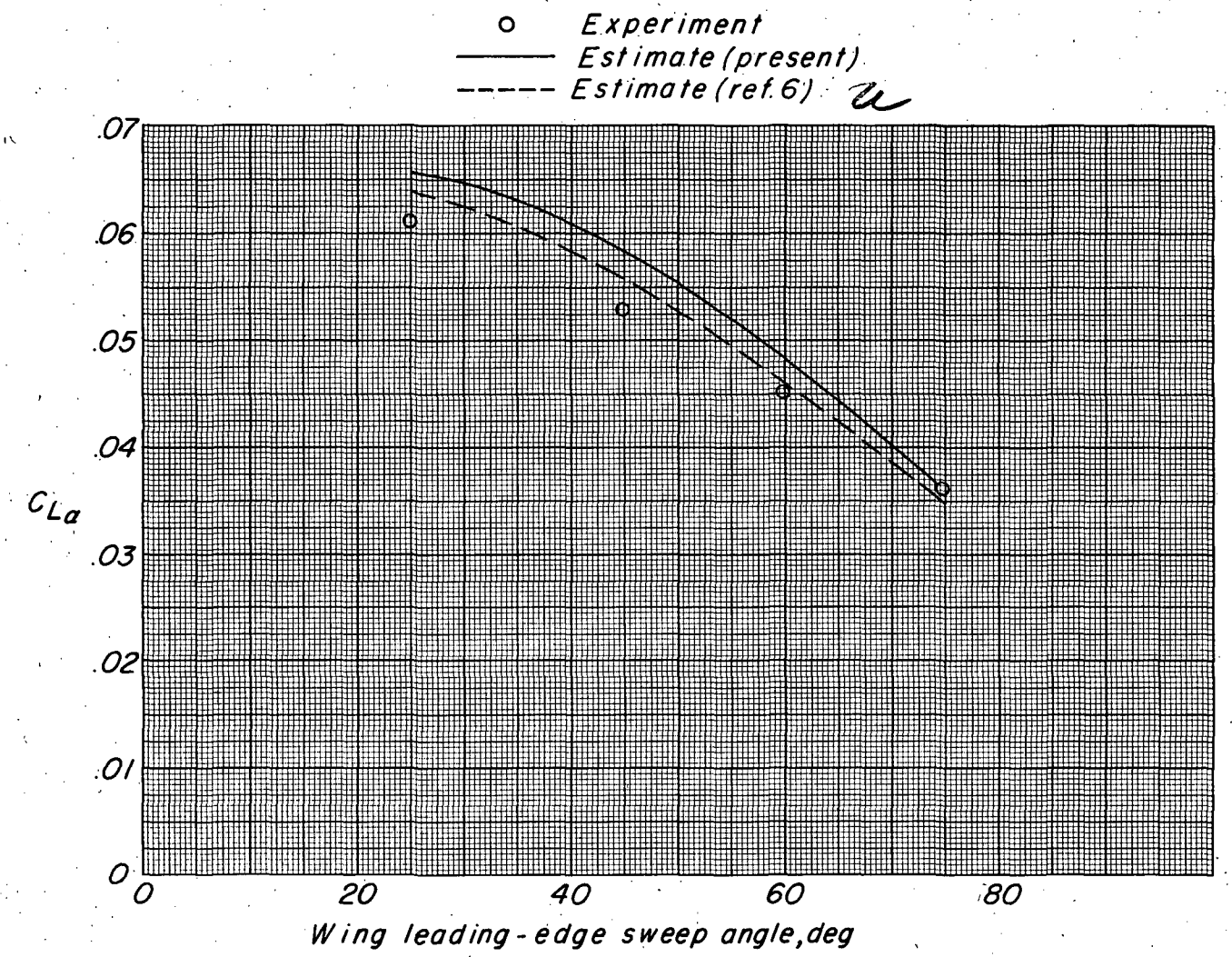

Figure 15.- Comparison of experimental and estimated values of lift-curve slope plotted against leading-edge sweep angle of outboard panel of configuration IV. $M \approx 0$.

Configuration		$\Lambda_{LE,in}$	Λ_{LE}	Aspect ratio
○	III	80°	80°	1.05
□	IV	60°	75°	1.89
◇	II	60°	60°	2.24
△	I	67.01°	61.7°	2.91
▷	IV	60°	60°	3.05
▱	IV	60°	45°	4.15
▯	IV	60°	25°	5.15
◇	III	80°	60°	5.26
◇	III	80°	40°	8.81
▱	III	80°	20°	10.35
▽	III	80°	0°	10.84

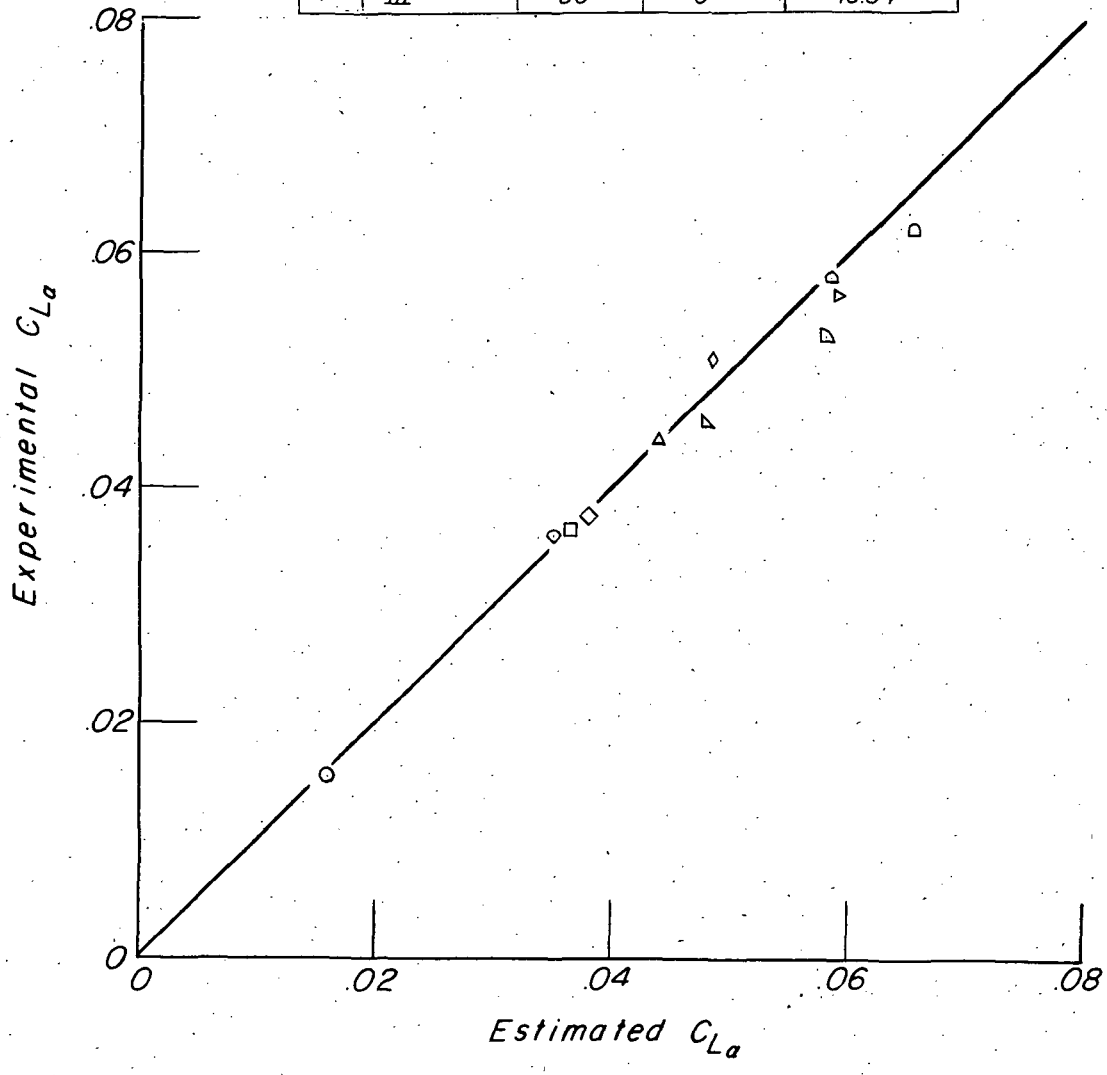

Figure 16.- Correlation of experimental and estimated values of lift-curve slope for configurations I to IV. $\alpha = 0°$.

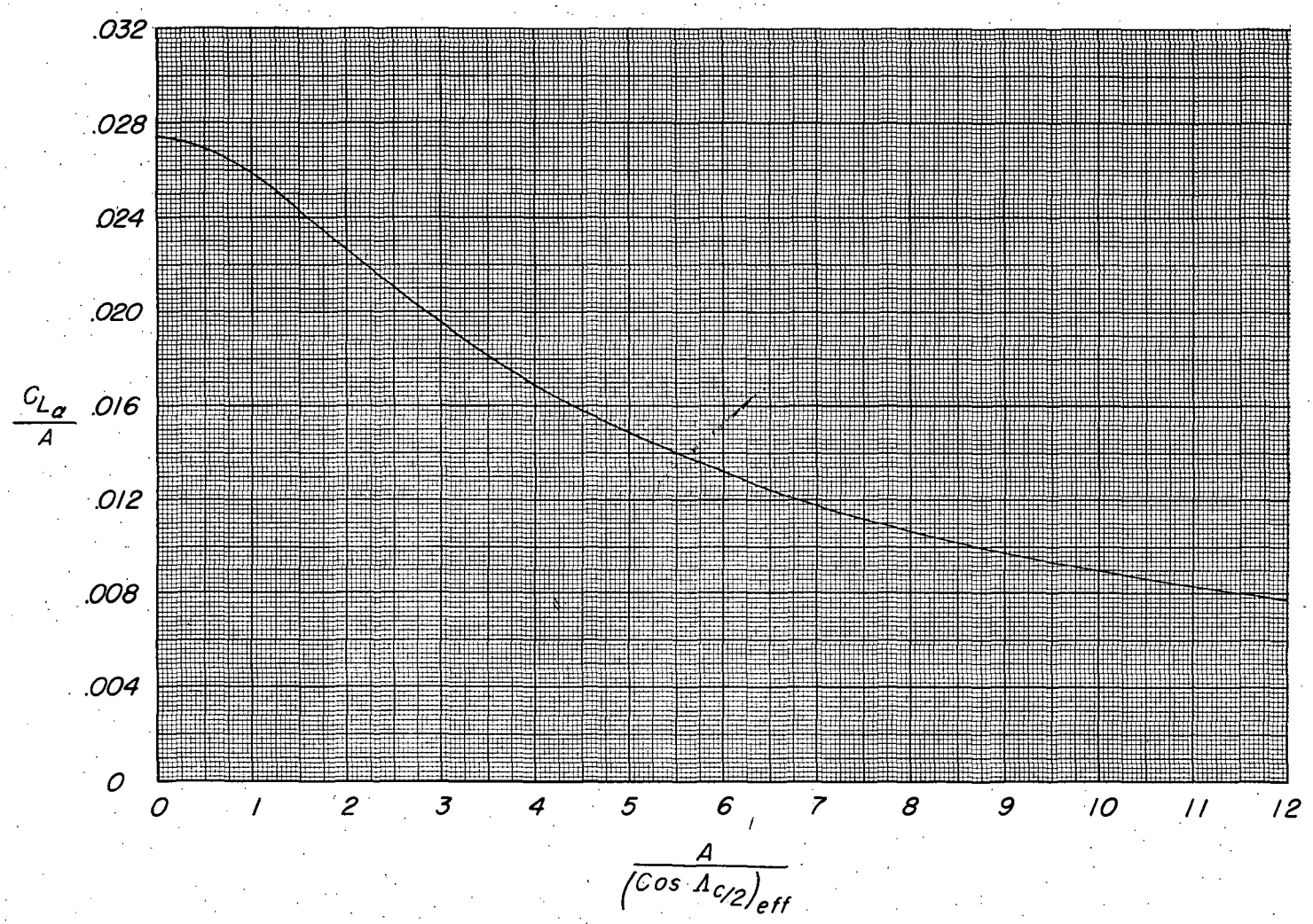

Figure 17.- Variation of $\frac{C_{L_\alpha}}{A}$ with $\frac{A}{(\cos \Lambda_{c/2})_{eff}}$ in incompressible flow.

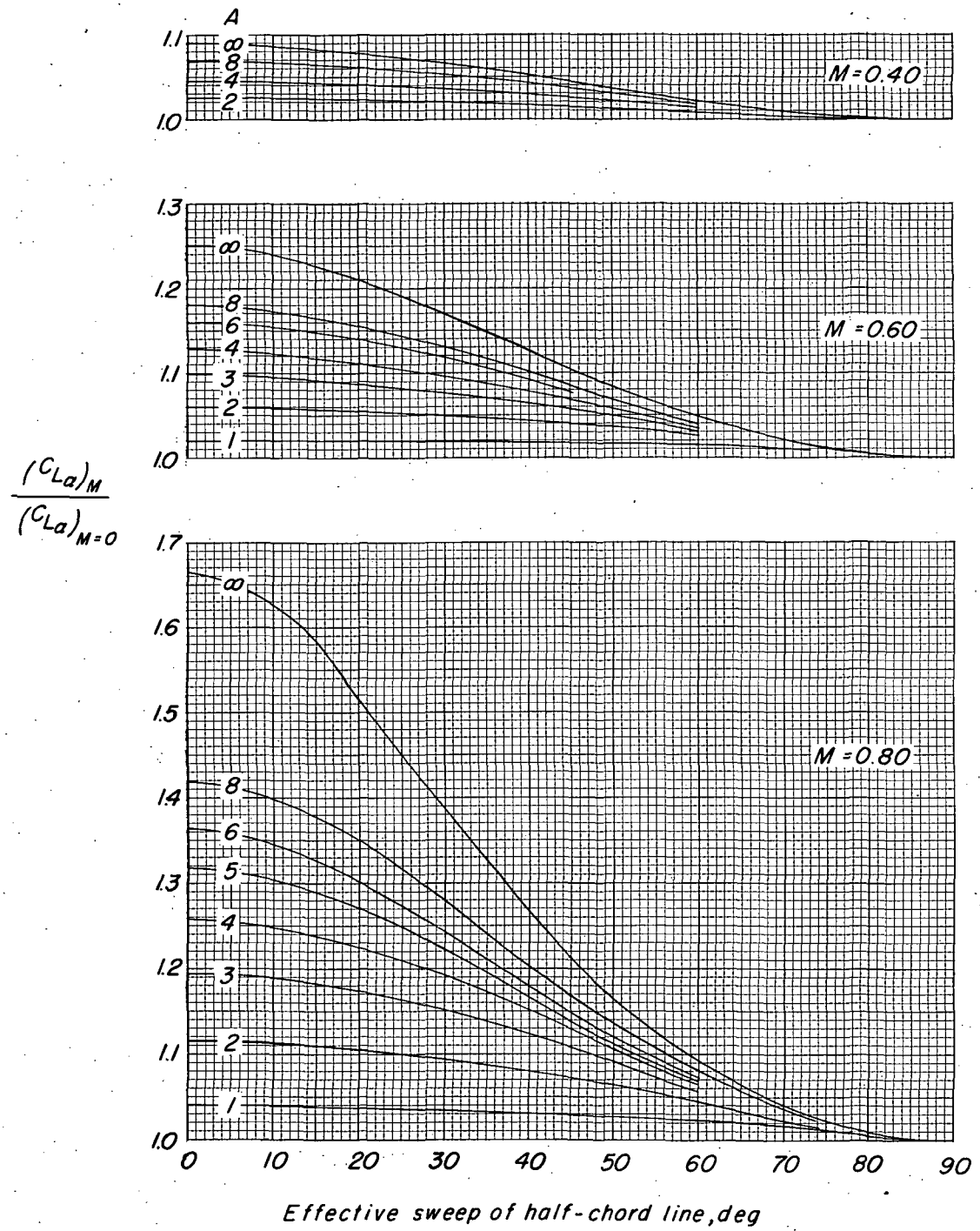

Figure 18.- Ratio of compressible to incompressible lift-curve slopes for subsonic speeds.

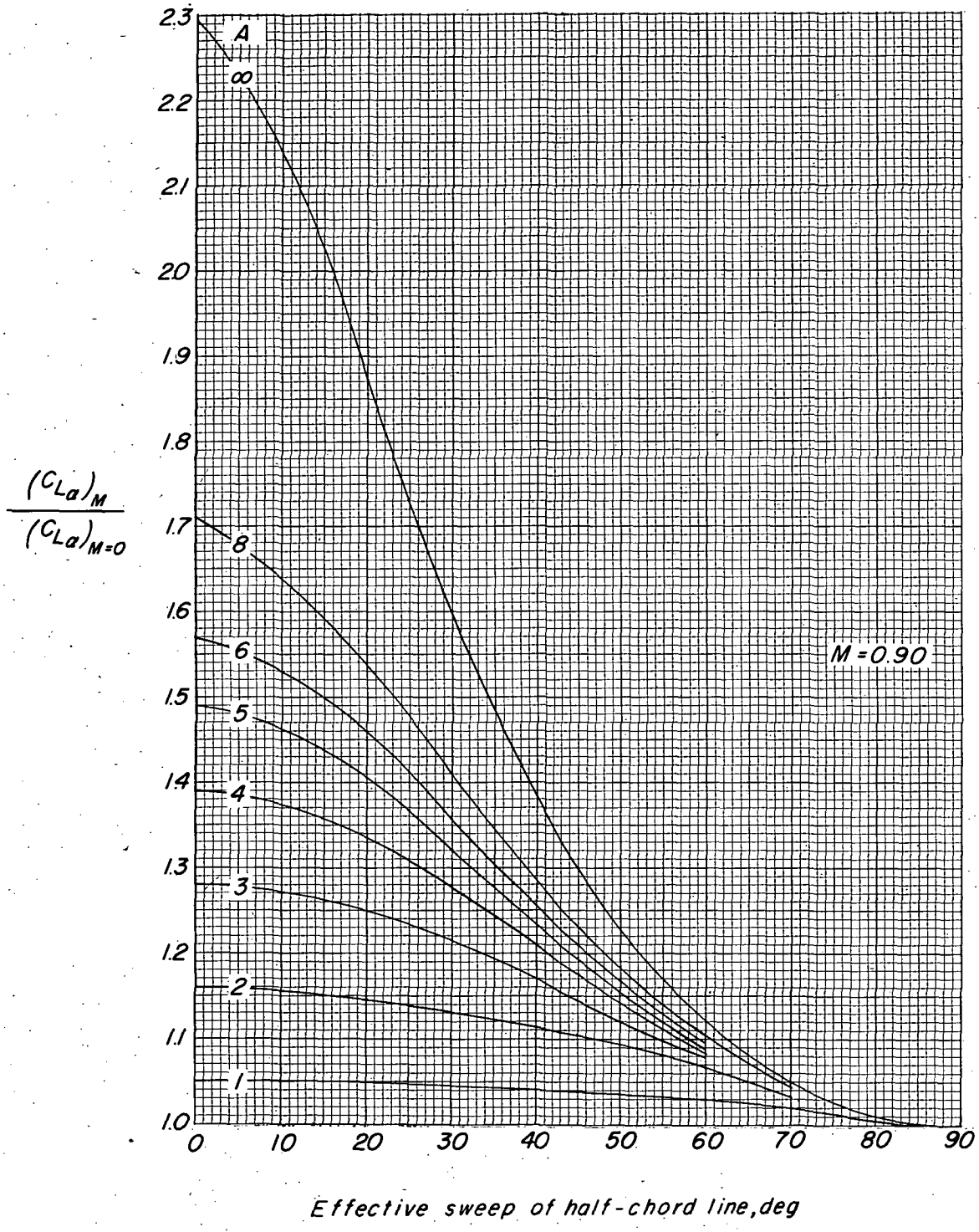

Figure 18.- Continued.

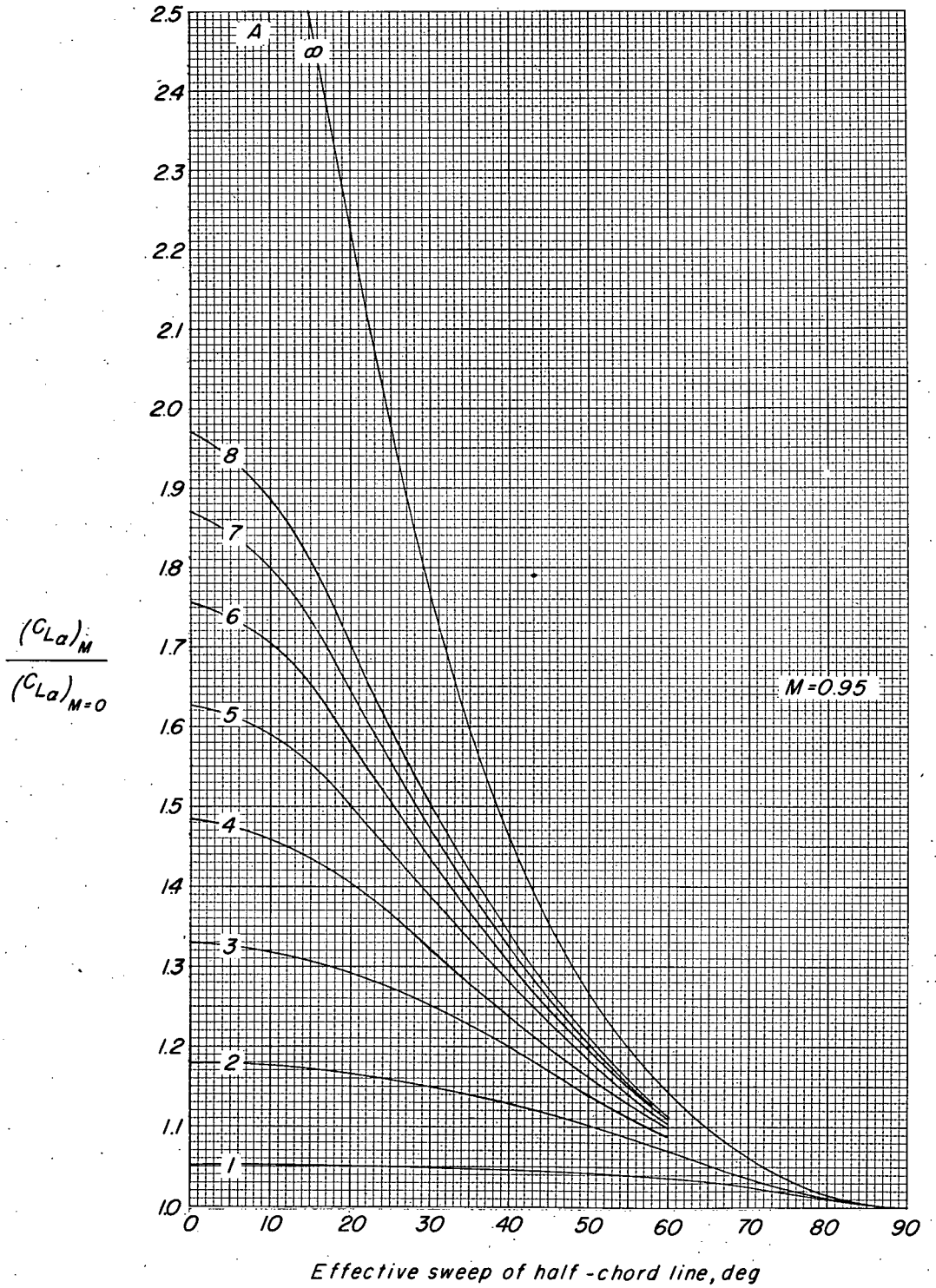

Figure 18.- Concluded.